Proceedings of the 21st ICSMGE, Vienna, Austria, 14 – 19 June 2026. Pistrol, Adam & Schweiger (eds.)
Published by: ÖGG, Austrian Society for Geomechanics, Salzburg, Austria, ISBN 978-3-9503898-4-5
https://doi.org/10.53243/ICSMGE2026-746

The effect of confining stress on the liquefaction resistance of two uniformly graded gravels with rounded and angular particles

Satuk Bugrahan Sari, Adda Athanasopoulos-Zekkos
Department of Civil and Environmental Engineering, University of California, Berkeley, U.S.A, satuk_sari@berkeley.edu

ABSTRACT: Previous studies have consistently demonstrated that, for a given cyclic stress ratio (CSR), soils tend to become more prone to cyclic liquefaction as the effective overburden stress increases. To address this, the correction factor K_σ is applied to normalize liquefaction resistance to a reference effective overburden stress of 1 atm, commonly used in empirical field databases, and to adjust empirical liquefaction resistance curves for conditions with overburden stresses either lower or, more importantly, higher than 1 atm. Despite its potential significance, the influence of high confining pressure on liquefaction resistance has received comparatively limited investigation, particularly in gravelly soils. This gap is amplified by the scarcity of documented liquefaction case histories for gravels relative to sands and silty sands. Prior work, such as Hynes and Olsen (1998) and Hynes et al. (2018), has suggested that many gravels exhibit a greater loss in cyclic strength at high confining stresses than sands, leading to potentially lower K_σ values. In contrast, this study presents results from large-scale cyclic simple shear (LSCSS) testing, using a 12-inch diameter device, on two uniform gravels with identical grain size distributions but differing particle angularities. Reconstituted loose ($D_R \approx 45\%$, prepared by air pluviation) and dense ($D_R \approx 85\%$, prepared by dry tamping) specimens were tested under confining stresses of 1, 2.5, 4, and 5.5 atm. Results indicate that, unlike many uniform sands, both gravels exhibit increased cyclic strength with higher confining pressure, though the magnitude of this increase depends on particle angularity. These findings highlight the need for caution when applying standard K_σ corrections to gravelly soils and suggest that tailored empirical or semi-empirical K_σ relationships should be developed for such materials, as their behavior can deviate substantially from that of sands.

KEYWORDS: Large scale cyclic simple shear testing, K_σ correction, gravel liquefaction.

1 INTRODUCTION

Liquefaction is a phenomenon in which saturated soil deposits experience a significant loss of stiffness and strength, typically as a result of rapid dynamic loading events such as earthquakes (Seed and Idriss, 1971). This reduction in shear resistance is driven by the progressive buildup of excess pore water pressures (Ishihara et al., 1975), which can lead to large strains in the soil mass and, in severe cases, catastrophic damage to infrastructure and threats to human safety.

A considerable body of research has examined the susceptibility of soils to liquefaction and the factors influencing liquefaction resistance (e.g., Bray and Sancio, 2006; Cao et al., 2011, 2013; Cubrinovski et al., 2018; Seed et al., 2003). Seed (1981) first introduced the concept of the K_σ factor, noting that the CSR required to reach a pore pressure ratio of 100% decreases as overburden pressure increases. Similarly, Seed et al., 2003 emphasized that susceptibility to liquefaction at a constant CSR increases with effective overburden stress, and that this effect must be accounted for separately from the normalization of field-based resistance indices such as Standard Penetration Test, Cone Penetration Test, or shear wave velocity.

In laboratory testing, liquefaction resistance is commonly represented by the cyclic resistance ratio (CRR), defined in cyclic simple shear tests as the ratio of cyclic shear stress (τ_{cyc}) to the initial vertical effective stress (σ'_{v0}), or in cyclic triaxial tests as τ_{cyc} divided by the effective confining stress (σ'_{vc}). CRR is typically reported for a specific number of loading cycles, N_c. Following Seed et al. (1975), who recommended $N_c = 15$ cycles for earthquakes with $M_w = 7.5$, this study uses CRR_{15} values when calculating corresponding K_σ values.

Equation (1) below illustrates the application of the correction factor K_σ to adjust the normalized liquefaction resistance for an initial effective overburden stress of 1 atm:

$$CRR_{15} = CRR_{15,1\ atm} \cdot K_\sigma \quad (1)$$

By rearranging this equation into Equation (2), K_σ can be determined in the laboratory as the ratio of the cyclic resistance ratio at a given overburden stress (commonly the consolidation or confining pressure in laboratory tests) to that at the reference overburden stress of 1 atm.

$$K_\sigma = \frac{CRR_{15}}{CRR_{15,1\ atm}} \quad (2)$$

Historically, the K_σ factor had limited influence on liquefaction triggering evaluations because field case histories tended to involve vertical effective stresses close to the reference 1 atm. As databases expanded, however, the importance of accounting for K_σ became clearer. Figure 1 below presents the recommendations of the NCEER Working Group (Youd et al., 2001) for applying the correction factor K_σ to adjust the normalized liquefaction resistance to an initial effective overburden stress of 1 atm.

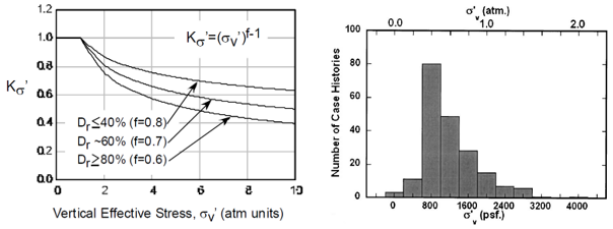

Figure 1. Recommendations for K_σ from the NCEER Working Group (Youd et al., 2001) and the range of vertical effective stresses observed in the field case history database (Cetin et al., 2004).

According to Youd et al. (2001), Equation (3) can be used for the correction factor K_σ as a function of vertical effective stress and relative density, where f is an exponent typically ranging from 0.6 to 0.8 depending on the relative density.

$$K_\sigma = (\sigma'_v)^{f-1} \quad (3)$$

The relationship between confining stress and liquefaction resistance is more apparent when plotted on a log-log scale. If the experimental data form a straight line on such a plot, it indicates that the data are well represented by a simple exponential function (Olsen, 1996). In this context, the exponent f corresponds to the slope of the trendline relating vertical effective stress (σ'_v) to liquefaction cyclic resistance (τ_{cyc}) in log-log space. Equivalently, the exponent f-1 in Equation (3) represents the slope of the vertical effective stress (σ'_v) versus cyclic resistance ratio (CRR) trendline, with opposite sign, in log-log scale.

Figure 2 provides an example of this concept for sandy soils. The stress focus (or point of convergence) shown is influenced by soil type and mineralogy, reflecting the tendency for resistance to converge at high confining stresses. For sandy soils, CRR_{1atm} generally increases with density, while the slope f decreases, leading to a reduction in K_σ.

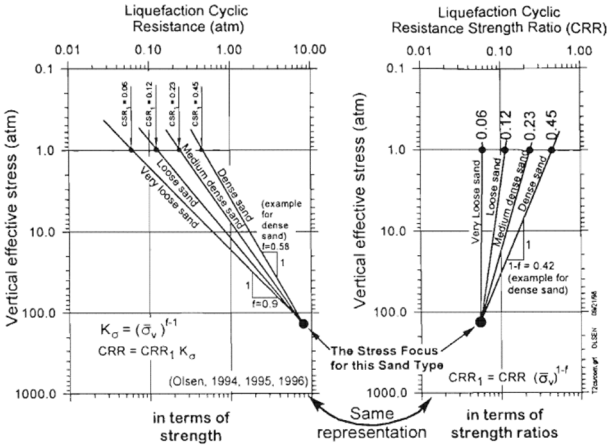

Figure 2. Determination of the exponent 1−f from log-log plots of vertical effective stress versus liquefaction resistance (Hynes and Olsen, 1998).

Referring to earlier studies, the observed decrease in normalized liquefaction resistance with increasing initial effective overburden stress (σ'_v) can be interpreted as a "critical state" behavior, where soils exhibit reduced dilatancy under higher effective stresses. Although the influence of overburden stress (i.e., the K_σ effect) has been demonstrated through laboratory tests by several researchers, including Vaid et al. (1985), Vaid and Sivathayalan (1996), and Hynes and Olsen (1998), most investigations have concentrated on sands or silty sands, which are commonly susceptible to liquefaction under loose conditions. Consequently, the impact of overburden stress on liquefaction triggering in gravelly soils remains less well understood, a situation that is understandable given the limited number of gravel liquefaction field case histories and the challenges associated with laboratory testing of gravelly soils due to their coarse grain size.

This study reports test results obtained using the Large Scale Cyclic Simple Shear (LSCSS) device, a distinctive prototype capable of testing gravel specimens up to 12 inches in diameter. Experiments were performed on two uniform gravels with identical grain size distributions but differing in particle angularity, designated as Rounded Uniform Gravel (RUG) and Angular Uniform Gravel (AUG). The outcomes for these materials are analyzed to evaluate the influence of particle angularity and vertical stress (i.e., confining or overburden stress) on liquefaction resistance.

2 TESTED MATERIALS

Laboratory tests on Rounded Uniform Gravel (RUG) and Angular Uniform Gravel (AUG), with properties summarized in Figure 6 and Table 1, were conducted using the unique Large Scale Cyclic Simple Shear (LSCSS) device at the University of California, Berkeley's GeoSystems Engineering Soil Mechanics Laboratory (Zekkos et al., 2018), shown in Figure 3. Reconstituted specimens, 12 inches (30.75 cm) in diameter, were prepared at two density levels: loose (approximately 45% relative density) using air pluviation, and dense (approximately 85% relative density) using dry tamping. These specimens were tested under various shear stresses. After consolidation, shear wave velocity (V_s) was measured for each specimen using accelerometers mounted on the device's top and bottom caps, with typical V_{s1} ranges for both densities reported in Table 1.

Figure 3. Large Scale Cyclic Simple Shear Device used for laboratory testing, University of California, Berkeley, GeoSystems Engineering Soil Mechanics Laboratory.

These two materials were intentionally chosen because they share many properties except for particle angularity, as illustrated in Figure 4. Their grain size distribution curves, shown in Figure 5, nearly overlap, with both materials having similar coefficients of uniformity $C_u = 1.4$. Despite the closely matching grain size distributions, the Rounded Uniform Gravel (RUG) consists of fully rounded particles with high sphericity, whereas the Angular Uniform Gravel (AUG) is composed of angular particles with low sphericity

(a) Rounded Uniform Gravel (RUG) *(b) Angular Uniform Gravel (AUG)*

Figure 4. Tested materials ($D_{50} \approx 17.4$-17.6 mm).

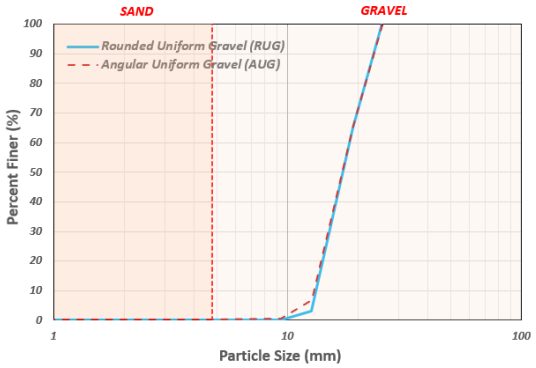

Figure 5. Grain size distribution of the tested materials.

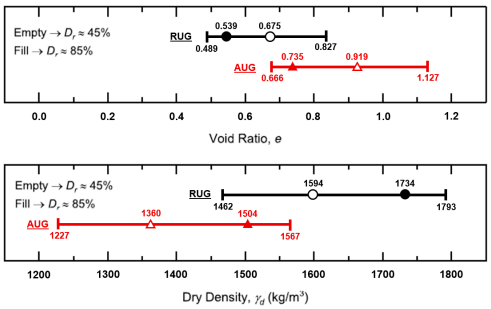

Figure 6. Ranges of void ratio and dry density of tested materials. $D_R \approx 45\%$ and 85% are shown within the ranges of maximum and minimum values of each material.

Table 1. Properties of the tested materials.

Tested Material	Soil Content (%)			USCS Class	G_s	D_{50} (mm)	C_u
	Fines	Sand	Gravel				
RUG	0	0	100	GP	2.67	17.6	1.4
AUG	0	0	100	GP	2.61	17.4	1.4

3 TESTING PROGRAM

As previously described, large-scale cyclic simple shear tests were conducted on reconstituted specimens of these two uniform granular materials at two density levels: loose (approximately 45% relative density), prepared by air pluviation, and dense (approximately 85% relative density), prepared by dry tamping. The specimens were subjected to shear under various confining stresses of 1, 2.5, 4, and 5.5 atm. For each density level, 3 to 4 cyclic tests were performed at each confining pressure. The shear load conditions (cyclic stress ratio, CSR) were selected to ensure at least one successful test with the number of cycles to liquefaction both below and above 15, as N_c=15 represents the typical number of cycles for an earthquake with moment magnitude 7.5 (Seed et al., 1975). Liquefaction was defined as occurring when the specimen's shear strain exceeded a single amplitude of 3.75%, a widely used criterion supported by previous studies (Kim et al., 2024; Hubler et al., 2017; Pillai and Stewart, 1994; Porcino et al., 2008; Sivathayalan, 2000; and Vaid and Sivathayalan, 1996). The cyclic frequency for all tests was set to 0.033 Hz (30 second cycle period), which has been shown to be appropriate for generating excess pore pressure in granular materials during cyclic loading.

Although all specimens have a nominal diameter of 307.5 mm, their heights vary between 116 and 120 mm depending on relative density and compaction. Displacements and stresses in both vertical and horizontal directions are measured using linear variable differential transformers (LVDTs) and load cells. Further detailed specifications of the large-scale cyclic simple shear device are available in Zekkos et al. (2018) and Kim et al. (2023).

The LSCSS device can perform cyclic shearing in either stress-controlled or strain-controlled modes using horizontal servo motors. In this study, all tests were conducted under stress-controlled conditions at specified shear load (CSR) levels. Shearing can be applied under either constant vertical load, simulating drained shear conditions, or constant volume, which represents undrained conditions. According to several studies, including Wai et al. (2022), maintaining constant volume during shear is crucial to accurately replicate undrained behavior typical of earthquake-induced liquefaction. While ASTM D6528-07 recommends limiting vertical strain to 0.05% to maintain constant volume, more recent research by Basham et al. (2019) and Zekkos et al. (2018), advocates for a stricter limit of 0.025%. The LSCSS device features an active feedback system to ensure constant volume, and all tests in this study complied with the 0.025% vertical strain threshold.

During cyclic shearing under constant volume conditions, specimens are prepared dry, and changes in vertical effective stress are interpreted macroscopically as equivalent to excess pore water pressure (EPWP) generation. This relationship, first established by Dyvik et al. (1987), has been widely adopted by many researchers (Nong et al., 2021; Hubler et al., 2017; Park et al., 2020; Kim et al., 2023, 2024; Chang et al., 2014; Zekkos et al., 2018; Boulanger and Seed, 1995; Vaid and Sivathayalan, 2000; Zehtab et al., 2019). That is, the change in vertical effective stress required to maintain constant specimen height and volume is considered to represent the excess pore pressure.

4 EXPERIMENTAL RESULTS

Two example test results are shown in Figure 7 below for both materials:

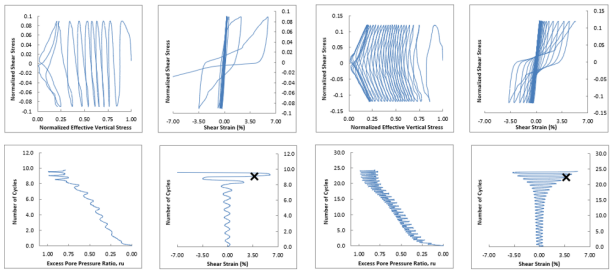

Test Material: *Rounded Uniform Gravel (RUG)*
Test ID: *TestRUG_L_400_0.09*
Relative Density: *45% (loose)*
Consolidation pressure: *400 kPa*
CSR: *0.09*
Nc: *10*

Test Material: *Angular Uniform Gravel (AUG)*
Test ID: *TestAUG_D_400_0.12*
Relative Density: *85% (dense)*
Consolidation pressure: *400 kPa*
CSR: *0.12*
Nc: *23*

Figure 7. Example test results for both materials.

Table 2 and Table 3 summarize the test results for both materials. The reported shear wave velocities correspond to the consolidation pressures for each test. The excess pore pressure coefficient, denoted as r_u in the final column, is given at a single amplitude shear strain of 3.75%. This coefficient is calculated as the ratio of excess pore pressure (i.e., the change in vertical effective stress during constant volume testing) to the initial vertical effective stress (σ'_{v0}), which is typically the consolidation or confining pressure in simple shear tests. These results are further illustrated in various plots across Figure 8 to Figure 12 to clearly present the findings.

Table 2. Cyclic simple shear test results for RUG.

State	Test ID	σ'_v	CSR	*V_s	**N_c	**r_u
		kPa	-	m/s	-	-
Loose ($D_R \approx$ 45%)	RUG_L_100_0.06	100	0.06	203	5	0.981
	RUG_L_100_0.05		0.05	240	17	0.922
	RUG_L_100_0.04		0.04	268	49	0.951
	RUG_L_250_0.08	250	0.08	305	7	0.915
	RUG_L_250_0.07		0.07	290	27	0.883
	RUG_L_250_0.06		0.06	287	37	0.977
	RUG_L_400_0.10	400	0.10	293	7	0.855
	RUG_L_400_0.09		0.09	297	10	0.869
	RUG_L_400_0.08		0.08	283	27	0.840
	RUG_L_550_0.12	550	0.12	308	7	0.778
	RUG_L_550_0.10		0.10	322	13	0.791
	RUG_L_550_0.08		0.08	319	39	0.936
Dense ($D_R \approx$ 85%)	RUG_D_100_0.08	100	0.08	258	7	0.889
	RUG_D_100_0.06		0.06	206	24	0.885
	RUG_D_100_0.04		0.04	231	71	0.937
	RUG_D_250_0.12	250	0.12	280	9	0.775
	RUG_D_250_0.10		0.10	274	17	0.811
	RUG_D_250_0.08		0.08	330	22	0.860
	RUG_D_250_0.06		0.06	318	80	0.939
	RUG_D_400_0.12	400	0.12	269	12	0.758
	RUG_D_400_0.10		0.10	334	22	0.846
	RUG_D_400_0.08		0.08	276	40	0.838
	RUG_D_550_0.14	550	0.14	317	9	0.763
	RUG_D_550_0.12		0.12	302	16	0.795
	RUG_D_550_0.10		0.10	298	27	0.768

Table 3. Cyclic simple shear test results for AUG.

State	Test ID	σ'_v	CSR	*V_s	**N_c	**r_u
		kPa	-	m/s	-	-
Loose ($D_R \approx$ 45%)	AUG_L_100_0.10	100	0.10	252	6	0.942
	AUG_L_100_0.08		0.08	219	17	0.942
	AUG_L_100_0.06		0.06	201	75	0.886
	AUG_L_250_0.12	250	0.12	265	2	0.818
	AUG_L_250_0.10		0.10	266	10	0.823
	AUG_L_250_0.08		0.08	279	29	0.864
	AUG_L_400_0.12	400	0.12	271	3	0.755
	AUG_L_400_0.10		0.10	307	13	0.841
	AUG_L_400_0.08		0.08	284	40	0.938
	AUG_L_550_0.12	550	0.12	311	5	0.833
	AUG_L_550_0.10		0.10	281	16	0.871
	AUG_L_550_0.08		0.08	317	50	0.825

Dense ($D_R \approx$ 85%)	AUG_D_100_0.14	100	0.14	244	3	0.852
	AUG_D_100_0.12		0.12	214	8	0.794
	AUG_D_100_0.10		0.10	236	20	0.840
	AUG_D_250_0.14	250	0.14	267	8	0.753
	AUG_D_250_0.12		0.12	265	14	0.770
	AUG_D_250_0.10		0.10	256	45	0.867
	AUG_D_400_0.16	400	0.16	275	4	0.723
	AUG_D_400_0.14		0.14	311	11	0.830
	AUG_D_400_0.12		0.12	299	23	0.803
	AUG_D_550_0.16	550	0.16	331	5	0.801
	AUG_D_550_0.14		0.14	316	15	0.770
	AUG_D_550_0.12		0.12	315	27	0.852

* Shear wave velocity measured at consolidation pressure, σ'_v
** Corresponds to γ=3.75% single amplitude shear strain

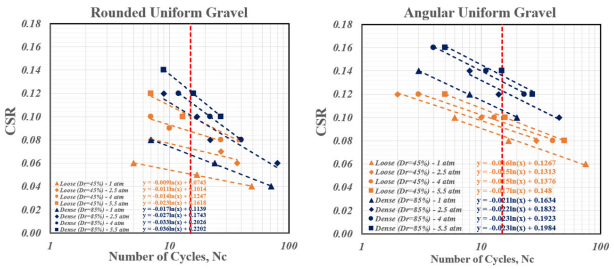

Figure 8. Number of cycles for liquefaction versus CSR plots for all tests (red vertical dashed line indicates N_c=15).

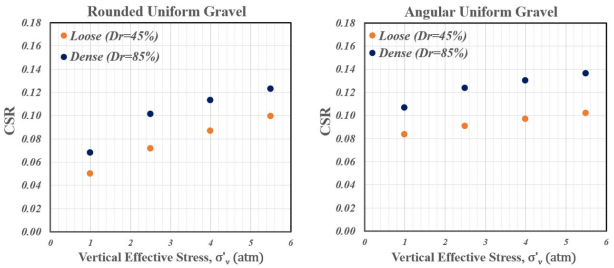

Figure 9. Vertical effective stress versus CSR data corresponding to N_c=15 (i.e., vertical effective stress vs. liquefaction resistance).

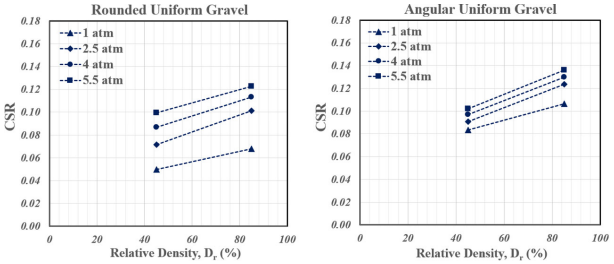

Figure 10. Relative density versus CSR data corresponding to N_c=15 (i.e., relative density vs. liquefaction resistance).

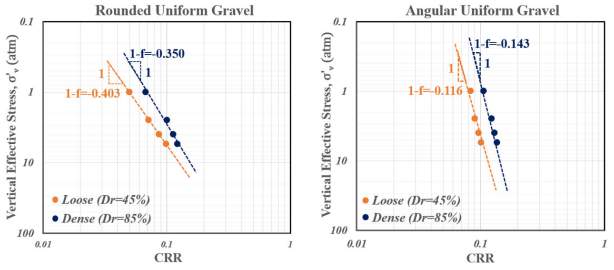

Figure 11. Log-log relationship between CRR and σ'_v.

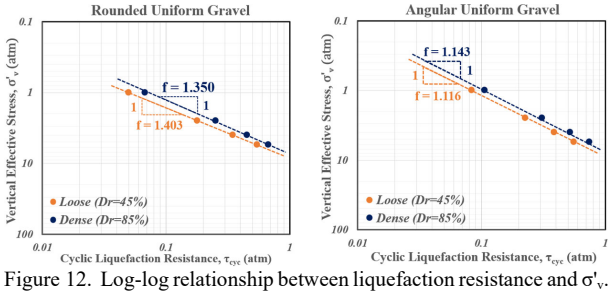

Figure 12. Log-log relationship between liquefaction resistance and σ'_v.

5 DISCUSSIONS AND CONCLUSIONS

In this study, two uniform gravel deposits, Rounded Uniform Gravel (RUG) and Angular Uniform Gravel (AUG), were tested using the Large Scale Cyclic Simple Shear (LSCSS) device under varying confining and shear stress conditions.

As illustrated in Figure 8, the angular gravel generally exhibits higher liquefaction resistance than the rounded gravel, particularly at lower confining pressures. Additionally, dense specimens ($D_R \approx$ 85%) show greater liquefaction resistance than loose specimens ($D_R \approx$ 45%) at the same vertical effective stress for both materials, which aligns with expectations. However, for Angular Uniform Gravel, the N_c - CSR relationships have comparable slopes for both loose and dense specimens, whereas for Rounded Uniform Gravel, the slope is less steep for loose specimens compared to dense ones. Figure 8 also reveals that, unlike most uniform sands reported in the literature, liquefaction resistance for both gravels increases with higher vertical effective stress. For example, in the rounded gravel, the CSR corresponding to 15 cycles is 0.100 (loose) and 0.123 (dense) at 5.5 atm vertical effective stress (orange and blue filled squares), decreasing to 0.050 (loose) and 0.068 (dense) at 1 atm (orange and blue filled triangles). Similarly, for the angular gravel, the CSR values are 0.102 (loose) and 0.136 (dense) at 5.5 atm, dropping to 0.083 (loose) and 0.107 (dense) at 1 atm.

This trend is more clearly illustrated in Figure 9, where the liquefaction resistances (CSR values corresponding to N_c = 15) are plotted against vertical effective stress for both materials. As shown, the data exhibit a positive slope, indicating that liquefaction resistance increases with higher vertical effective stress, opposite to the behavior typically observed in uniform sands.

The influence of density on liquefaction resistance is evident in Figure 10, where CSR values are plotted against relative density for all confining pressures. For both materials, dense specimens ($D_R \approx$ 85%) exhibit greater liquefaction resistance than loose specimens ($D_R \approx$ 45%) at the same vertical effective stress, resulting in positive slopes for all trendlines. In both materials, the 1 atm tests (triangles) appear at the bottom, representing the lowest liquefaction resistance, while the 5.5 atm tests (squares) are positioned at the top, indicating the highest resistance. The figure also shows that for Angular Uniform Gravel, liquefaction resistances across all confining pressures are closer in value compared to those for Rounded Uniform Gravel. This narrower range results in smaller K_σ values (closer to 1) for the angular material, since K_σ is defined as the ratio of liquefaction resistance at any confining pressure to that at the 1 atm reference pressure.

Because liquefaction resistance increases with vertical effective stress for both uniform gravels, K_σ values rise above 1 as confining pressure increases. Based on this trend, K_σ correction factors as functions of vertical effective stress were developed for both materials, as illustrated in Figure 13.

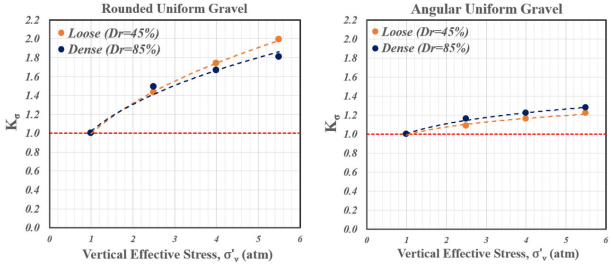

Figure 13. Recommended K_σ correction factors for both materials.

As shown in Figure 13, K_σ values exceed 1 for both materials, indicating that liquefaction resistance increases with confining

pressure. Whereas uniform sands typically lose about 10-30% of their resistance at higher confining pressures, these two uniform gravels exhibit resistance gains of approximately 20-100% at elevated vertical effective stresses.

The figure also demonstrates that the strength gain is more pronounced for the rounded material compared to the angular one, suggesting that particle angularity has a diminishing effect on strength gain with increasing confining pressure. In fact, AUG is more resistant to liquefaction compared to RUG as shown in Figure 8 because angular grains boost liquefaction resistance with more efficient particle locking during cyclic loading. Nevertheless, the rounded material exhibits a greater relative increase in strength than the angular one with increasing vertical effective stress as illustrated in Figure 13 due to more efficient packing of rounded grains under higher confining pressures compared to angular ones. Cubrinovski and Ishihara (2002) states that the void ratio of the densest possible packing, i.e., e_{min}, can best be achieved with perfect spheres, leading to the idea that rounded particles are prone to more efficient packing under high confining pressures. Angular particles, on the other hand, are less efficient in packing since more gaps would remain between the grains no matter how high the confining pressure is, assuming no particle crushing. This efficient packing behavior of RUG compared to AUG ends up with smaller void ratios under high confining stresses, leading to a more pronounced relative strength gain (i.e., higher K_σ values) for the rounded material under higher pressures, and illustrating the reverse effect of particle angularity on K_σ correction factor.

As discussed earlier, Youd et al. (2001) recommends using Equation (3) to determine the correction factor K_σ as a function of vertical effective stress, where f is an exponent typically ranging from 0.6 to 0.8 depending on relative density. This exponent f corresponds to the slope of the vertical effective stress (σ'_v) versus liquefaction cyclic resistance (τ_{cyc}) trendline in log-log space. In other words, the exponent f-1 in Equation (3) represents the slope of the σ'_v - cyclic resistance ratio (CRR) trendline, with opposite sign, in log-log scale. For the tests conducted in this study, the corresponding log-log plots are shown in Figure 11 and Figure 12. The cyclic liquefaction resistance (τ_{cyc}) values were obtained by multiplying the CRR values by their corresponding vertical effective stresses (σ'_v), and these results are summarized in Table 4 for both materials.

Table 4. Liquefaction resistance at varying confining pressures for both materials.

σ'_v (atm)	CSR at N_c=15				τ_{cyc} at N_c=15 (atm)			
	Loose (D_R≈45%)		Dense (D_R≈85%)		Loose (D_R≈45%)		Dense (D_R≈85%)	
	RUG	AUG	RUG	AUG	RUG	AUG	RUG	AUG
1	0.050	0.083	0.068	0.107	0.050	0.083	0.068	0.107
2.5	0.072	0.091	0.101	0.124	0.179	0.227	0.253	0.309
4	0.087	0.097	0.113	0.130	0.347	0.388	0.453	0.520
5.5	0.100	0.102	0.123	0.136	0.547	0.561	0.675	0.749

For the observed trend of increasing K_σ and liquefaction resistance with increasing vertical effective stress in both uniform gravels, the exponent f in Figure 12 is greater than 1. Consequently, the 1−f exponent in Figure 11 becomes negative and can be applied in Equation (3) after reversing its sign. This negative 1−f exponent corresponds to the negative slope in Figure 11 as CRR increases along the horizontal axis.

For both soil deposits, the relationship between confining stress and liquefaction resistance is more clearly observed on a log-log scale. In fact, the experimental data for both materials align almost as straight lines in this scale, indicating that the relationship is well described by a simple exponential curve, as suggested by Olsen (1996). The stress focus, i.e., the point of convergence introduced in Figure 2 to illustrate the tendency of liquefaction resistance to converge at high confining stresses, can be readily envisioned in Figure 11 and Figure 12 for $\sigma'_v >$ 5.5 atm, which was the maximum pressure tested in this study.

In conclusion, the findings of this study highlight the need for caution when applying the K_σ correction to the liquefaction resistance of gravelly soils. Although the tests conducted on two uniform gravel types are insufficient to draw broad conclusions for all gravelly soils, nearly all existing literature does not recommend $K_\sigma > 1$ at high confining pressures for gravels. While adopting $K_\sigma \leq 1$ at elevated confining pressures offers a conservative and safe approach by assuming reduced liquefaction resistance, presuming a decrease where resistance actually increases contradicts sound engineering judgment and critical thinking, potentially leading to uneconomical designs. Hence, it is essential and strongly advised to develop gravel-specific empirical or semi-empirical K_σ estimation models by examining soil properties that influence liquefaction resistance, as gravel behavior may differ significantly from similar sands.

6 REFERENCES

ASTM. 2006. Standard Test Method for Consolidated Undrained Direct Simple Shear Testing of Cohesive Soils. *ASTM D6528-07. West Conshohocken, PA: ASTM.*

Boulanger, R. W., and Seed, R. B. 1995. Liquefaction of sand under bidirectional monotonic and cyclic loading. *J. Geotech. Eng.* 121 (12): 870–878. https://doi.org/10.1061/(ASCE)0733-9410(1995)121:12(870).

Bray, J. D., and Sancio, R. B. 2006. Assessment of the liquefaction susceptibility of fine-grained soils. *J. Geotech. Geoenviron. Eng.* 132 (9): 1165–1177. https://doi.org/10.1061/(ASCE)1090-0241(2006)132:9(1165).

Cao, Z., Youd, T. L., and Yuan, X. 2011. Gravelly soils that liquefied during 2008 Wenchuan, China earthquake, Ms=8.0. *Soil Dyn. Earthquake Eng.* 31 (8): 1132–1143. https://doi.org/10.1016/j.soildyn.2011.04.001.

Cao, Z., Youd, T. L., and Yuan, X. 2013. Chinese dynamic penetration test for liquefaction evaluation in gravelly soils. *J. Geotech. Geoenviron. Eng.* 139 (8): 1320–1333. https://doi.org/10.1061/(ASCE)GT.1943-5606.0000857.

Cetin, K. O., Seed, R. B., Der Kiureghian, A., Tokimatsu, K., Harder Jr, L. F., Kayen, R. E., & Moss, R. E. 2004. Standard penetration test-based probabilistic and deterministic assessment of seismic soil liquefaction potential. *Journal of geotechnical and geoenvironmental engineering,* 130(12), 1314-1340.

Chang, W. J., Chang, C. W., and Zeng, J. K. 2014. Liquefaction characteristics of gap-graded gravelly soils in K_0 condition. *Soil Dyn. Earthquake Eng.* 56 (Jan): 74–85. https://doi.org/10.1016/j.soildyn.2013.10.00.

Cubrinovski, M. and Ishihara, K. 2002. Maximum and minimum void ratio characteristics of sands. *Soils and foundations*, *42*(6), 65-78.

Cubrinovski, M., Bray, J. D., C. de la Torre, Olsen, M., Bradley, B., Chiaro, G., Stocks, E., Wotherspoon, L., and Krall, T. 2018. Liquefaction- induced damage and CPT characterization of the reclamations at CentrePort, WellingtonLiquefaction-induced damage and CPT Characterization of the Reclamations at CentrePort,Wellington. *Bull. Seismol. Soc. Am.* 108 (3B): 1695–1708. https://doi.org/10.1785/0120170246.

Dyvik, R., Berre, T., Lacasse, S., and Raadim, B. 1987. Comparison of truly undrained and constant volume direct simple shear tests. *Géotechnique* 37 (1): 3–10. https://doi.org/10.1680/geot.1987.37.1.3.

Hubler, J. F., Athanasopoulos-Zekkos, A., and Zekkos, D. 2017. Monotonic, cyclic, and postcyclic simple shear response of three uniform gravels in constant volume conditions. *J. Geotech. Geoenviron. Eng.* 143 (9): 04017043. https://doi.org/10.1061/(ASCE)GT.1943-5606.0001723.

Hynes, M. E., and Olsen, R. 1998. Influence of confining stress on liquefaction resistance. *Proc., International Symposium on the Physics and Mechanics of Liquefaction, Balkema, Rotterdam, The Netherlands, 145–152.*

Hynes, M. E., and Olsen, R. S. 2018. Influence of confining stress on liquefaction resistance. *In Physics and mechanics of soil liquefaction (pp. 145-151). Routledge.*

Ishihara, K., Tatsuoka, F., and Yasuda, S. 1975. Undrained deformation and liquefaction of sand under cyclic stresses. *Soils and foundations*, *15*(1), 29-44.

Kim, J., Athanasopoulos-Zekkos, A., and Cubrinovski, M. 2023. Monotonic and cyclic simple shear response of well-graded sandy gravel soils from Wellington, New Zealand. *J. Geotech. Geoenviron. Eng.* 149 (7): 04023046. https://doi.org/10.1061/JGGEFK.GTENG-10619.

Kim, J., Athanasopoulos-Zekkos, A., and Zekkos, D. 2024. The Effect of Initial Static Shear Stress on Liquefaction Triggering of Coarse-Grained Materials. *Journal of Geotechnical and Geoenvironmental Engineering*, *150*(10), 04024099.

Nong, Z.-Z., Park, S.-S., and Lee, D.-E. 2021. Comparison of sand liquefaction in cyclic triaxial and simple shear tests. *Soils Found. 61 (4):* 1071–1085. https://doi.org/10.1016/j.sandf.2021.05.002.

Olsen, R. S. 1996. The influence of confining stress on Liquefaction Resistance. *In First US-Japan Workshop on Advanced Research on Earthquake Engineering for Dams. 12-14 November 1996* (p. 193).

Park, S.-S., Nong, Z.-Z., and Lee, D.-E. 2020. Effect of vertical effective and initial static shear stresses on the liquefaction resistance of sands in cyclic direct simple shear tests. *Soils Found.* 60 (6): 1588–1607. https://doi.org/10.1016/j.sandf.2020.09.007.

Pillai, V., and Stewart, R. 1994. Evaluation of liquefaction potential of foundation soils at Duncan Dam. *Can. Geotech. J.* 31 (6): 951–966. https://doi.org/10.1139/t94-110.

Porcino, D., Caridi, G., and Ghionna, V. 2008. Undrained monotonic and cyclic simple shear behaviour of carbonate sand. *Géotechnique 58* (8): 635–644. https://doi.org/10.1680/geot.2007.00036.

Seed, H. B. 1981. Earthquake-resistant design of earth dams.

Seed, H., Idriss, I., Makdisi, F., and Banerjee, N. 1975. Representation of irregular stress time histories by equivalent uniform stress series in liquefaction analyses. *EERC 75-29. Berkeley, CA: Earthquake Engineering Research Center, Univ. of California, Berkeley.*

Seed, R. B., et al. 2003. Recent advances in soil liquefaction engineering: A unified and consistent framework. *In Proc., 26th Annual ASCE Los Angeles Geotechnical Spring Seminar. Reston, VA: ASCE.*

Seed, H. B., and Idriss, I. M. 1971. Simplified procedure for evaluating soil liquefaction potential. *Journal of the Soil Mechanics and Foundations division*, *97*(9), 1249-1273.

Sivathayalan, S. 2000. Fabric, initial state and stress path effects on liquefaction susceptibility of sands. *Ph.D. dissertation, Dept. of Civil Engineering, Univ. of British Columbia.* https://doi.org/10.14288/1.0063762.

Vaid, Y., and Chern, J. 1985. Cyclic and monotonic undrained response of saturated sands. *In Proc., Advances in the Art of Testing Soils under Cyclic Conditions. Reston, VA: ASCE.*

Vaid, Y., and Sivathayalan, S. 1996. Static and cyclic liquefaction potential of Fraser Delta sand in simple shear and triaxial tests. *Can. Geotech. J.* 33 (2): 281–289. https://doi.org/10.1139/t96-007.

Vaid, Y. P., and Sivathayalan, S. 2000. Fundamental factors affecting liquefaction susceptibility of sands. *Can. Geotech. J.* 37 (3): 592–606. https://doi.org/10.1139/t00-040.

Wai, D., Manmatharajan, M. V., and Ghafghazi, M. 2022. Effects of imperfect simple shear test boundary conditions on monotonic and cyclic measurements in sand. *J. Geotech. Geoenviron. Eng.* 148 (1): 04021164. https://doi.org/10.1061/(ASCE)GT.1943-5606.0002682.

Youd, T. L., et al. 2001. Liquefaction resistance of soils; summary report from the 1996 NCEER and 1998 NCEER/NSF workshops on evaluation of liquefaction resistance of soils. *J. Geotech. Geoenviron. Eng.*, 127(10), 817–833.

Zehtab, K., Gokyer, S. S.Werden, Marr, A.W., and Apostolov, A. 2019. On the effects of inadequate height control in constant volume monotonic and cyclic direct simple shear test. *In Proc., Eighth Int. Conf. on Case Histories in Geotechnical Engineering. Reston, VA: ASCE.* https://doi.org/10.1061/9780784482100.037.

Zekkos, D., Athanasopoulos-Zekkos, A., Hubler, J., Fei, X., Zehtab, K. H., and Marr, W. A. 2018. Development of a large-size cyclic direct simple shear device for characterization of ground materials with oversized particles. *Geotechnical Testing Journal*, 41(2), 263-279.